

## Response to reviewer 1

The authors thank the reviewer for their constructive comments, our responses to each individual point can be found below:

Changes to the manuscript in line with the responses are outlined in blue:

This technical note compares different methods to quantify hysteresis patterns and introduces a new, more robust way to do so. The manuscript is well-organized, clearly written and potentially of interest to quite some of the readers. From my point of view, it can be considered for publication after addressing a few minor comments:

(1) although being widely used in hydrology, the term "hysteresis" used here is formally incorrect. Hysteresis is defined as the dependence of a system output on its history of inputs (and thus on its internal state). Although discharge is a manifestation of the system state, the discharge-concentration relationships are technically no hysteresis loops but rather closed loops of a functional relationship. In addition, actual hysteresis is characterized by unique input-output relationships below and above given threshold values (e.g. Schmitt-triggers from electronic circuits as examples for sharp hysteresis). I would therefore suggest to qualify the terminology here, for example by stating:"[...] closed loops, thereafter referred to as hysteresis loops".

As the reviewer says, the term hysteresis is widely used in hydrology and is generally understood by the hydrological community. As a result the authors do not think it is necessary to add an additional explanation.

(2) p.7883, l.9ff: I could not quite follow this explanation. In other words, I am not sure if the new method is capable of a more robust representation of figure-of-eight shapes. Even if using the normalized ranges, wouldn't a regular 8-shape (for the sake of the argument say for example horizontally aligned at an angle of 0 degrees) result in a HI of 0 in spite of exhibiting "hysteresis"? It would be great if the authors elaborated a bit on that and clarified this question.

Yes, we agree that this point needs clarifying in the manuscript. The reviewer is correct in saying that a regular symmetrical figure-of-8 loop (i.e. equal size loops on either side) would result in an HI index of 0. But that is a simple fact of an unbiased loop. The new index however, does allow the method of quantification to consider the portions of the loop which are in clockwise or anti-clockwise phase and this information could be extracted for further evaluation. This is an improvement on the previous published hysteresis indices. If the new index is used in conjunction with other existing hysteresis measures such as loop area, it is easy for the user to see that a loop which has a HI of 0 but a loop area which is larger than 0 has to exhibit figure-of-8 behaviour. In addition to this, because the calculation of the new index uses multiple sections across the loop, which will encompass the clockwise and anti-clockwise sections, it is possible to examine the distribution of values gained for the index before they are averaged, thus allowing the user to see the value of the index in each section of the loop. Text will be added to the technical note to clarify that users who are examining figure-of-eight loops may find it helpful to use the new index in conjunction with other loop measures and/or visual examination of the loop shape to ensure an effective interpretation of the results. So to be clear, here we focus on the basic output that can be generated. Once implemented other summary results can be gained that can be used to highlight different aspects of the loop characteristics (one could summarise separately the +/- aspects of the loops for more complex behaviour). This is beyond our technical note, but we shall briefly note that other characteristics can be quantified as this is a strength of the new methodology.

Text has been added to the manuscript lines 193-203

(3) is there a particular reason not to show the box plots in figure two with equal y-axis scales (at least for panel ii and iv of each storm). this could more clearly illustrate that HI<sub>new</sub> is somewhat more robust.

Yes, we shall modify the plots so that the y-axes match in each of the ii and iv panels for ease of comparison.

Plots have been modified, however, due to the fact that the index can only produce a number between -1 and 0 (unlike the original index), so all the y-axes in panel iv have been made consistently between -1 and 1.

## Response to reviewer 2

Thank you for these useful comments, our response to each of the points raised can be found below:

This technical note gives a review of some indices that are used to describe direction and magnitude of hysteretic relationships between discharge and concentration and proposes a new hysteresis index. Hysteretic relationships between concentration (geochemical tracers, nutrients) and discharge or also between storage (i.e. moisture contained within a control volume) and discharge have been used to describe catchment functioning and to compare catchments or different time periods. Observed hysteretic behavior could help to infer flow processes and better understand runoff generation. In that respect, this technical note, although more geared in its current scope towards nutrient and sediment export from (agricultural) catchments, could be interesting for many readers dealing with hillslope and catchment hydrological processes. This technical note is well-written and mostly clear in its explanations and structure

I understand that a technical note has to be brief. Still, I would recommend to provide a short explanation in the introduction of what is meant by hysteresis in this context and to elaborate a bit on the value of a hysteresis index (HI). Why can it be a useful descriptor of catchment functioning? Has the examination of hysteresis patterns advanced process understanding? How can it help to pinpoint release mechanisms for nutrients or sediments beyond a mere comparison of numbers between catchments? What does it mean if a hysteretic loop is clockwise or anti-clockwise in terms of processes? This also refers to the conclusions section where authors state that the new HI could “become a standardized analytical technique to be used by the water quality research community”.

The authors appreciate that some of this background information could be useful to the reader and can help support the value of using a HI, however they are also conscious of the need for brevity in a technical note. Therefore the authors propose that a sentence can be added to the technical note which refers the reader to an additional paper which is currently in press which uses the new hysteresis index as a tool for quantifying hysteresis loops across different parameters and field sites. This paper covers in detail all of the issues you highlight here in your comment and would allow the reader to see how the hysteresis index can be used. We ask for advice from the Editor on the basis this is a technical note paper and such discussion should be limited.

Text has been added to provide additional background and a definition of hysteresis in the introduction (lines 29-32), also details of what different hysteresis pattern mean in terms of processes (lines 44-50). An extra recommendation has been added to the conclusions section, along with an expanded explanation of why the index is of wider significance for the hydrological community (lines 241-244).

P. 7879, L 3: Please explain TNU

NTU is a standard unit of measurement of turbidity which stands for “Nephelometric Turbidity Units”. This could be added to the manuscript, however we would argue that this abbreviation is widely accepted and commonly used in the hydro-chemical literature. We are happy to clarify this though.

Has been added to the manuscript (line 96)

P. 7879, L 19-21: Please make the explanation of the calculation of the adapted HI clearer. What exactly does it mean to calculate HI “at every 25, 10% etc of the discharge” and to calculate for different “sections” (e.g. p. 7884, L 15-19) or use different “increments”. This remained somewhat unclear to me throughout the text.

The original index proposed by Lawler et al. 2006 used the mid-point in discharge to determine the measurement point for the index (50% of the discharge range). Our adapted and new method instead determines multiple locations across the loop at which to measure the strength of the hysteresis. Therefore we tested the impact of using different numbers of measuring points or increments, including every 25% of the discharge range i.e. 3 equally spaced measurement increments across the loop, 10% of the discharge range (9 increments) etc... If helpful a visual aid could be produced and added to the methodology section to clarify this difference but we believed this was clear in the current text and presentation.

A visual aid has been added in the form of figure 3.

P. 7881, L 25 – p. 7882, L 4: redundant, as it is explained in the figure caption

Agreed, this can be removed as it is repeated in the figure caption.

Has been removed.

P. 7883, L 7-14: this description belongs to methods (section 2.3), not results

The description of the new index is covered in the methodology section, however, in the results the details are reiterated in order to clearly explain what the reader is observing in the figure. Therefore the authors would like the sentence to remain.

P. 7884, L 6-7: meaning of sentence unclear

Agreed, this sentence will be amended to read: “This technique is useful when the user’s interest is in the relative characteristics of the loop geometries”.

Amended as above

p. 7884, L 7: “These” means these recommendations?

Yes, should be these recommendations, text can be modified to clarify.

Has been modified.

### Response to reviewer 3

The technical note from Lloyd et al. (“Testing an improved index for analysing storm nutrient hysteresis”) compares methods for calculating a hysteresis index for concentration - discharge relationships during storm events. The note is appropriate for HESS and will be of interest to researchers seeking metrics to interpret C-Q relationships. My only major recommendation is that

the authors remove "nutrient" from the title since the paper does not discuss nutrient data (but rather turbidity - discharge relationships).

Thank you for your comment. We agree with your recommendation; we therefore propose to amend the title to "Technical Note: Testing an improved index for analysing storm hysteresis dynamics". We use turbidity as an example in the technical note, as hysteresis in turbidity is prevalent in the literature and we had a large number of storms displaying a wide range of hysteretic behaviours for which we could test our methodology (explained P7879 ln3-6), however the technique is more widely applicable to any quantifiable water quality parameter. We would like therefore to represent this in a broader title.

Following additional constructive advice from the editor, the title has been amended to "Technical Note: Testing an improved index for analysing storm discharge- concentration hysteresis."

Response to reviewer: Remi Dupas

Thank you for your comments, our response to the individual points you raise can be found below:

This technical note reviews some of the hysteresis-descriptor variables used to analyse high frequency storm concentration time series. Two major shortcomings of the widely used hysteresis index (Lawler et al., 2006) are highlighted: the influence of initial concentration and of initial discharge in the case of 8-shaped hysteresis. A new hysteresis index is presented to overcome these two shortcomings. It worth noting that this is one of the rare studies where uncertainty in the data is accounted for in classifying hysteresis loops. This technical note is well-written, logically organized, and the figures are clear. This technical note would benefit from two major improvements

(1) An alternative method already exist to deal with the problems of changing baseline value and 8-shaped hysteresis loops. See Rossi et al. (2005) and also Stutter et al. (2008) and Dupas et al. (2015) for examples of application. Here is an extract from Stutter et al. (2008): "Further analyses were undertaken using the 'pollutogram' approach developed by Rossi et al. (2005) approximated by the relationship:  $F(x)=x^{\beta}$  where  $F(x)$  is the fraction of the total mass of the determinant during the storm event and  $x$  is the total mass of water during the event. The parameter  $\beta$  is a coefficient representing the relationship between the mass and water volume over time which may be plotted as the cumulative proportion of the total mass transported against the cumulative proportion of water transported. Values of  $\beta$  of 1 indicate that the determinant mass arrived predominantly towards the start, or end of the event, respectively. A value of  $\beta = 1$  denotes either that the pollutant mass and water volumes are proportional, or that the pollutant concentrations stay constant over the event." Maybe mention this method.

Thank you for this suggestion. There are a number of different methods which can be used to examine storm behaviours, some of which we have discussed in this technical note. The method you describe is another viable method for examining storm behaviour, however the pollutogram is designed to examine discharge-load relationship, which are subtly different to discharge-concentration relationships. This is important in our work as we consider variables such as turbidity from which a load cannot be directly calculated unless converted to suspended sediment. With this in mind, the authors would prefer not to add this method to our discussion as we only wish to include methods which directly examine discharge-concentration relationships as we have indeed identified in the introduction to the paper.

(2) Maybe mention the fact that the new HI gives a description the size and direction of the biggest loop in the case of a 8-shaped loop but the information that it is a 'figure-of-eight' is lost. See also comment (2) Anonymous Referee #1. The method mentioned in (1) leads to the same information loss.

Please see the response provided to Reviewer 1 (comment 2). In brief, the new index provides a useful method for quantification which reflects the proportion of the loop which is in clockwise and anti-clockwise phase in the case of figure-of-8 loops. If the index is coupled with a visual inspection of the loops, then no information is lost, or indeed if the information is extracted separately from each loop as noted here: 1) If the value obtained for the HI is small but other metrics such as loop area are large in comparison, then it can quickly be determined that the loop is a figure-of-eight. 2) In addition, the multiple sections of the loop which are measured as part of the index calculation can be examined before they are averaged, and therefore a switching between positive and negative values indicates the switching from clockwise to anti-clockwise behaviour, resulting in a figure-of-8. The amendments proposed in response to comments made by reviewer 1 should also help to clarify the point raised here and will we add text to note these additional behaviours that can be quantified as another positive aspect of the new approach.

[See earlier response and modifications](#)

Minor comments:

P 7876 l2: "in extreme flow events" -> why not all storm events?

Agreed, this could apply to any storm events, text will be modified.

[Text in the abstract has been amended to storm events.](#)

P 7877 l14: a major interest of hysteresis-descriptor variables is that they enable statistical analysis of near continuous high-frequency measurements, when the amount of data exceeds the capacity of manual analysis.

Agreed, the hysteresis index therefore is a useful tool, and if it is used along-side other metrics such as loop-area it can provide detailed information about the loop shape without having to visually examine each loop. See comments above and in response to reviewer 1.

[See earlier response and modifications](#)

P 7881 l20-22: the hysteresis shapes are already described before using the method presented in the paper. Maybe specify that this is based on preliminary visual observation of discharge-concentration plots.

Yes, this is based on visual inspection, this was done to ensure that a large range of loop shape and sizes were available to thoroughly test the proposed new method. Text will be added to clarify this point.

[Text has been added lines 153-154](#)

1 **Technical Note: Testing an improved index for analysing storm ~~nutrient hysteresis discharge-~~**  
2 **concentration hysteresis.**

3 Lloyd, C.E.M.<sup>1,2</sup>, Freer, J.E.<sup>2</sup>, Johnes, P.J.<sup>2</sup> and Collins, A.L.<sup>3</sup>

4 <sup>1</sup> School of Chemistry, University of Bristol, Cantock's Close, Bristol, BS8 1TS, UK.

5 <sup>2</sup> School of Geographical Sciences, University of Bristol, University Road, Bristol, BS8 1SS, UK.

6 <sup>3</sup>Department of Sustainable Soils and Grassland Systems, Rothamsted Research, North Wyke,  
7 Okehampton, EX20 2SB, UK

8 \* Corresponding author: Charlotte Lloyd

9 Address: School of Chemistry, University of Bristol, Cantock's Close, Bristol, BS8 1TS, UK.

10 e-mail: [charlotte.lloyd@bristol.ac.uk](mailto:charlotte.lloyd@bristol.ac.uk)

11 Telephone: +44 (0)117 3316795 Fax: +44 (0)117 927 7985

12  
13 *Abstract*

14 Analysis of hydrochemical behaviour ~~in extreme flow~~during storm events can provide new insights  
15 into the process controls on nutrient transport in catchments. The examination of storm behaviours  
16 using hysteresis analysis has increased in recent years, partly due to the increased availability of high  
17 temporal resolution datasets for discharge and **nutrient parameters**. A number of these analyses  
18 involve the use of an index to describe the characteristics of a hysteresis loop in order to compare  
19 ~~different~~ storm behaviours both within and between catchments. This technical note reviews the  
20 methods for calculation of the hysteresis index (HI) and explores a new more effective methodology.  
21 Each method is systematically tested and the impact of the chosen calculation on the results is  
22 examined. Recommendations are made regarding the most effective method of calculating a HI  
23 which can be used for comparing data between storms and between **different parameters** and  
24 catchments.

25

26 *1. Introduction*

27 The analysis of hysteresis patterns is a key tool for the interrogation of in-stream physical and  
28 chemical responses to storm events, which have been shown to be important periods for the  
29 transport of nutrients and sediment within catchments (Bowes et al., 2003;Jarvie et al., 2002;Jordan  
30 et al., 2007;Burt et al., 2015;Evans and Johnes, 2004). In the context of this paper, hysteresis is  
31 defined as the nonlinear relationship between discharge and concentration of nutrients or sediment.

32 When discharge-concentration data are plotted a cyclic pattern is often observed, the strength of  
33 the relationship is dependent on the nature of the lag in response between the two variables.

34 Quantification of hysteresis allows multiple storm behaviours to be examined between and within  
35 catchments, for a wide range of hydrological and hydrochemical parameters. This can provide insight  
36 into catchment function, allowing the development and testing of process-based understanding.

37 This type of analysis has been used in recent years by many authors investigating nutrient  
38 concentration-discharge relationships in catchments of differing environmental character (e.g.  
39 Bowes et al., 2015;Darwiche-Criado et al., 2015;Cerro et al., 2014;Rodriguez-Blanco et al.,  
40 2013;Oeurng et al., 2010;Eder et al., 2010;Evans and Johnes, 2004) but, traditionally, has been used  
41 for the examination of turbidity or suspended sediment data (e.g. Ziegler et al., 2014;House and  
42 Warwick, 1998;Williams, 1989;Tena et al., 2014;Klein, 1984;Whiting et al., 1999). Hysteresis analysis  
43 has been used to support the investigation of the temporal variations in nutrient transport to  
44 streams as a means of characterising the likely contributing source areas and flow pathways linking  
45 source to stream in complex landscapes (Outram et al., 2014;Bowes et al., 2015;Lloyd et al., 2016).

46 Similar hysteresis patterns can be observed for a variety of different reasons, however it is generally  
47 assumed that clockwise hysteresis, caused by a small or no lag between discharge and concentration  
48 suggests a source close to the monitoring point. Conversely, anti-clockwise hysteresis generally  
49 signifies a longer lag between the discharge and concentration peak, suggesting that the source was  
50 located further from the monitoring point. (Williams, 1989) provides a detailed summary of different  
51 shape hysteresis plot and the possible mechanisms.

52 For hysteresis analysis to be effective and easy to interpret there is a need to develop an effective  
53 method of classifying storms according to their hysteretic behaviour. Many papers have classified  
54 storms into clockwise or anticlockwise responses, and described the strength of the hysteresis as  
55 small or large (Bowes et al., 2015;Evans and Davies, 1998;Butturini et al., 2008). Other authors have  
56 used an index approach, which allows a dimensionless quantification of the hysteresis, and thus,  
57 comparison of hysteresis indices between catchments of differing size, morphology and hydrological  
58 function. An index approach is also useful as it provides information about both the direction and  
59 strength of the hysteresis. Hysteretic indices proposed by Butturini et al. (2008) provide semi-

60 quantitative methods to describe whether the measured parameter is enriched or diluted during a  
61 storm event and to assess the area inside the hysteresis loop, along with its direction. Langlois et al.  
62 (2005) propose a quantitative method which involves splitting the discharge hydrograph into the  
63 rising and falling limb and fitting regression lines to each dataset. The hysteresis index is calculated  
64 as the ratio (rising:falling) of the areas under the regression curves. Whilst this index provides a  
65 quantitative solution, the authors suggest that the method should only be applied to simple uni-  
66 directional loops, i.e. not those which exhibit figure-of-eight or more complex behaviours. A  
67 quantitative index was also proposed by Lawler et al. (2006), which uses the ratio of the turbidity (or  
68 other parameter) concentration on the rising and falling limb, at the mid-point in the discharge. The  
69 mid-point in discharge is defined as 50% of the range in discharge during the storm event. This index  
70 has been used by a number of other authors (McDonald and Lamoureux, 2009; Outram et al., 2014),  
71 as it is flexible and can be applied to hysteresis loops of all shapes. However it is not without  
72 limitations. In a recent paper, Aich et al. (2014) highlight that the index of Lawler et al. (2006) in its  
73 current form becomes skewed at higher concentrations, with a smaller index calculated for loops of  
74 the same shape and area in the case of storms commencing at a higher concentration (Figure 1a). In  
75 addition, the calculation of the index using only the mid-point (50%) in discharge can be problematic.  
76 Lawler et al. (2006) state that the mid-point was used as it avoids the often noisy sections at the  
77 beginning and end of the loops. However, the result of the calculated index may be misleading in  
78 many figure-of-eight scenarios, especially those which cross close to the mid-point in discharge (see  
79 Figure 1b). The example shown in Figure 1b illustrates that a hysteresis index (HI) calculated at the  
80 mid-point in discharge would suggest that there was very little hysteresis, even though there is a  
81 strong effect but in different directions during different periods of the storm event. As suggested by  
82 Lawler et al. (2006), the HI can be calculated at multiple increments through the flow range and an  
83 average HI value gained. Against the above background, this technical note reports the impact of the  
84 chosen method on the index values generated from a series of storms of varying size and hysteretic  
85 shapes, using an adapted version of the Lawler et al. (2006) index ( $HI_{LA}$ ). The paper also introduces a  
86 new method for calculating the hysteresis index ( $HI_{new}$ ) and, as a result of this analysis, suggests a  
87 recommendation for the most appropriate calculation for a HI for storm-driven nutrient transport in  
88 catchments.

## 89 *2. Methodology*

### 90 *2.1 Datasets*

91 The example uses a series of storms extracted from high-temporal resolution (15-min) data collected  
92 on the River Wylfe at Brixton Deverill (Wiltshire, UK) as part of the Defra Demonstration Test



93 Catchment project (McGonigle et al., 2014) from March 2012 to March 2014. Detailed descriptions  
94 of the field site and the datasets are available in previously published work (Lloyd et al., 2015, in  
95 revision). For the purposes of this study, discharge data were obtained from the Environment  
96 Agency gauge (Gauge Number 43806) and turbidity data were collected using a YSI 6-series sonde,  
97 which was cleaned and calibrated once a month over the monitoring period. Turbidity (measured in  
98 Nephelometric Turbidity Units (NTU)) was chosen for this study as it is the most widely examined  
99 parameter in terms of hysteresis and the storms selected from the data set exhibit a wide range of  
100 turbidity values and hysteretic shapes. A total of 66 storms were extracted for this analysis from the  
101 two year observational data. A storm was classified as an increase in discharge of more than 20%  
102 above baseflow and the end of the storm was determined by either a return to baseflow conditions  
103 or when discharge began to rise again if another storm occurred before the system had returned to  
104 baseflow conditions. Previous work had quantified the uncertainty associated with the discharge and  
105 turbidity measurements (Lloyd et al., 2015; Lloyd et al., submitted) (Lloyd et al., 2015; Lloyd et al.,  
106 2016) and this provided 100 resampled iterations of each measured parameter for every storm,  
107 accounting for observational uncertainties, for this analysis. Figure 2a-f(l) shows some example  
108 storms, where the boxes represent the 5<sup>th</sup>- 95<sup>th</sup> percentile uncertainty range for each data point.

## 109 2.2 Lawler et al. (2006) method and modification

110 The HI was then calculated according to the standard method of Lawler et al. (2006) ( $HI_L$ ) for  
111 combinations of all 100 iterations of each of the storms to provide a distribution of HI when the mid-  
112 point in discharge was calculated (50%). The Lawler et al. (2006) method was also adapted ( $HI_{LA}$ ),  
113 where HI was calculated at every 25%, 10%, 5% and 1% increments of the discharge (see Figure 3 for  
114 visualisation) as shown below:

115 if  $T_{RL} > T_{FL}$  (clockwise hysteresis):

$$116 \quad HI_L = \left( \frac{T_{RL}}{T_{FL}} \right) - 1 \quad (1)$$

117 Or, if  $T_{RL} < T_{FL}$  (anti-clockwise hysteresis):

$$118 \quad HI_L = \left( -1 / \frac{T_{RL}}{T_{FL}} \right) + 1 \quad (2)$$

119

120 Where:  $T_{RL}$  is the value of turbidity at a given point in flow on the rising limb and  $T_{FL}$  is the value on  
121 the falling limb.

122 When multiple sections per storm were calculated, the average value was taken to represent the HI  
123 of the complete storm event. In some cases there were not corresponding values on both the falling  
124 and rising limbs, when this occurs the maximum number of available pairs of data were used to  
125 calculate the index. This **only usually** occurred at lowest discharges and when a large number of  
126 intervals were being analysed. This meant that the number of missing pairs was small compared with  
127 the available pairs (<5%) and as a result had little impact on the overall calculation. The analyses  
128 were completed for both the raw data and for normalised storms to assess the impact of the  
129 different analysis methods on the HI values obtained. The data were normalised using the following  
130 equations:

$$131 \quad \text{Normalised } Q_i = \frac{Q_i - Q_{min}}{Q_{max} - Q_{min}} \quad (3)$$

$$132 \quad \text{Normalised } T_i = \frac{T_i - T_{min}}{T_{max} - T_{min}} \quad (4)$$

133 Where:  $Q_i/T_i$  is the discharge/turbidity at timestep  $i$ ,  $Q_{min}/T_{min}$  is the minimum storm parameter value  
134 and  $Q_{max}/T_{max}$  is the maximum storm parameter value.

### 135 2.3 Proposed new Hysteresis Index method ( $HI_{new}$ )

136 A new method of calculating a HI was also tested ( $HI_{new}$ ) with the aim of eliminating the impact of a  
137 changing baseline value on the ratio as multiple measurements are taken from the same storm. The  
138 new index uses the difference between the turbidity values on the rising and falling limbs of the  
139 normalised storms, rather than a ratio, and effectively normalises the rising limb at every  
140 measurement point, thereby resulting in an index between -1 and 1.

$$141 \quad HI_{new} = T_{RL_{norm}} - T_{FL_{norm}} \quad (5)$$

142 As with the other methods, the analysis was carried out using different intervals of discharge (25%,  
143 10%, 5% and 1% ) and the mean was used as the final HI value for the storm. The impact of this  
144 number of chosen intervals of discharge on the magnitude of the resulting HI was tested.

145 The resulting distributions of HI values for each method were then scrutinised using boxplots.  
146 Differences between the distributions of data for each storm were analysed statistically using  
147 ANOVA where normality and variance assumptions were met, and the non-parametric alternative  
148 Kruskal-Wallis-H on ranked data where the ANOVA assumptions did not hold. When a significant  
149 difference between the groups was detected, a pairwise Tukey test was used to establish which of  
150 the groups were contributing to the effect. The main aim of the analysis was to determine the point  
151 at which sufficient intervals of discharge were used so that there was no statistically significant  
152 difference between the different datasets for each storm.

153 3. Results and discussion

154 A total of 66 storms were analysed using the three methods for calculating the HI, which included 35  
155 anti-clockwise loops, 11 clockwise loops, 12 figure-of-eight loops which were mainly anti-clockwise  
156 and, 8 figure-of-eight loops which were mainly clockwise (loop shapes were examined by visual  
157 inspection). The peak turbidity during the storms ranged between 10 and 392 NTU (mean = 91 NTU)  
158 and the starting values were between 2 and 31 NTU (mean = 8 NTU). Figure 2 shows six example  
159 storms (a-f, panel I) from the range of behaviour identified above, each with varying shape and size.  
160 ~~Figure 2a-f (panel II) shows the distribution of values for the calculated H-index using  $H_L$  (measured~~  
161 ~~at 50% of discharge range) and the  $H_{LA}$  (measured at varying percentile increments of discharge).~~  
162 ~~The grey areas on the plots show the boxplots which were not statistically different from one~~  
163 ~~another, that is, there is no gain by increasing the number of intervals of discharge measured for~~  
164 ~~that storm.~~ Table 1 summarises the number (and percentage) of storms tested which can be  
165 adequately represented by the different discharge interval frequencies tested.

166 Figure 2a-f(II) shows the distributions of HI values (using  $H_L$ ) measured at only 50% of discharge are  
167 often very different from the analyses which measure multiple sections across the loop ( $H_{LA}$ ). The  
168 more complex the shape of the loop, the more measured sections are needed to represent it  
169 adequately. The analysis shows that by using 5% increments of discharge (19 sections), 98% of the  
170 storms analysed showed stable distributions and therefore no significant changes were observed  
171 when additional increments were included. While including more increments of the loop in the  
172 analysis does improve the HI results, it does not solve all of the issues highlighted earlier. Both  $H_L$   
173 and  $H_{LA}$  are sensitive to the size of the storm and, as a result, for a similar pattern in hysteresis but a  
174 larger magnitude of storm, a comparatively smaller value would be calculated for the index, as  
175 shown in Figure 1a. This means that the results generated for a series of storms are very difficult to  
176 interpret and it is difficult to compare between individual storms and catchments. By normalising  
177 the storms as described above and continuing to use the  $H_{LA}$  method, the comparability of the  
178 outputs between storms is improved as they are all assessed on the same scale. However, if multiple  
179 increments of discharge are included, which has been shown to be beneficial, then effectively each  
180 of the individual measured sections of the storm need to be normalised, otherwise the problem is  
181 reduced but not eradicated. This problem is illustrated in Figure 1c, which shows an example of an  
182 idealised and normalised storm where the width of the loop remains constant through most of the  
183 storm. However at different quantiles of flow, HI value varies due to the loop gradient, the HI is  
184 inflated towards the lower and reduced at higher quantiles of discharge. The  $H_{new}$  was designed to  
185 overcome this problem. The new index uses the range of turbidity values between the rising and

186 falling limb at each increment of discharge rather than the ratio, thereby directly quantifying the  
187 width of the loop.

188 Figure 43 shows how the new index effectively normalises the rising limb and examines the relative  
189 behaviour of the falling limb, thereby identifying the proportion of the storm occurring in a clockwise  
190 or anti-clockwise phase. For this new method to be robust, it is necessary to normalise the data as  
191 described earlier before the analysis. Figure 2a-f(III) show the example storms in their normalised  
192 forms. The new index produces a value between -1 and 1, where 0 represents no hysteretic pattern  
193 and positive values clockwise and negative values, anti-clockwise hysteresis. A figure-of-eight storm  
194 will be represented as a weighted average of the intervals of discharge measured when the storm  
195 was in a clockwise phase and when it was in an anticlockwise phase. Therefore, for example, if the  
196 storm exhibits anti-clockwise behaviour for a large proportion of the storm event the average  $HI_{new}$   
197 will produce a negative number. It should be noted that in the unusual case that an exactly  
198 symmetrical figure-of-eight storm is presented the index would produce a value of 0, suggesting no  
199 hysteresis. Using the HI value in conjunction with loop area will however provide clarification as a  
200 storm which has an HI of 0 but a positive loop area has to be a complex loop shape. The advantage  
201 with our new technique is that the user can choose to interrogate other output metrics within these  
202 results, such as the quantified loop area and the distribution of HI values calculated for each section  
203 of the loop in addition to the averaged HI value. By looking at the distribution of values it is simple to  
204 identify complex loop shapes such as figure-of-eight (due to both positive and negative values  
205 calculated for the various loop sections) and ensures correct interpretation of the HI values.  
206 Although we do not explore the advantage of these further analyses here, we suggest they  
207 potentially provide a richer analyses of hysteresis dynamics that we aim to explore in future papers.

208 We suggest tThe new index provides a consistent approach to the core loop characteristics and  
209 therefore is more easily interpretable by the user when comparing behaviour between storms or  
210 field sites. Figure 2a-f(IV) show the resulting distributions of  $HI_{new}$  generated using varying  
211 increments of discharge. The analysis shows that the distribution of calculated values was generally  
212 more stable compared with the  $HI_{LA}$  method and, in many cases, fewer increments of discharge were  
213 necessary to produce a statistically stable representation of the storm loop shape (Table 1). The  
214 results demonstrate that increasing the increments to every 10% of discharge allowed 95% of storms  
215 and using 5% increments allows 100% of storms to be robustly characterised in terms of their loop  
216 shape, meaning that the addition of more sections did not significantly alter the distribution of HI  
217 results.

218 *4. Conclusions and recommendations*

219 The concept of using an index to aid the quantification of storm hysteresis has been established for  
220 over two decades. However few papers have chosen to use them, perhaps due to the limitations  
221 associated with the most common methods. This technical note was designed to test systematically,  
222 for the first time, the way that the HI is calculated and to quantify the impact of the chosen method  
223 on the results. The analysis has led to a number of recommendations concerning how the HI should  
224 be calculated in order to produce results which are both statistically robust and comparable  
225 between storms and field sites. This technique is useful when the user's interest is in the relative  
226 characteristics of the loop geometries~~This technique is useful when the interest and interpretation is~~  
227 ~~in the core relative characteristics of the loop geometries themselves~~. These recommendations are:

- 228 1. Storms should be normalised before analysis so that multiple storms can be robustly  
229 compared.
- 230 2. A range method, such as the new index ( $HI_{new}$ ) proposed here, should be used in preference  
231 to a ratio method as it produces results which are easier to interpret, allowing quantification  
232 of the extent of the hysteresis effect that can be directly compared between contrasting  
233 catchments even when the magnitude of the storms varies greatly.
- 234 3. Multiple sections of each loop should be analysed so that the extent and direction of the  
235 hysteresis can be accounted for throughout the flow range. Sections should be measured at  
236 least every 10% of the discharge range, although every 5% is recommended as it is likely,  
237 based on our analysis, to produce robust results for almost all storm sizes and shapes.
- 238 3.4. Examine the distribution of HI values calculated across the sections in addition to the  
239 averaged value, as this aids robust classification of complex loop shapes, including figure-of-  
240 eight loops.

241 Undertaking the analysis of hysteresis loops using these guidelines improves the clarity of the  
242 hysteresis index as a diagnostic tool for the analysis of storms and how discharge-concentration  
243 patterns vary. The new index ( $HI_{new}$ ) is able to describe robustly the shape and direction of a  
244 hysteretic pattern in storms of any size, and can be used to compare storms from multiple  
245 catchments. This means that the index becomes more useful as it has the potential to become a  
246 standardised analytical technique that can be utilised by the water quality research community.  
247 Lloyd et al. (2016) illustrates the use of the new hysteresis index to investigate storm behaviours  
248 across different nutrient parameters and between contrasting catchments. This study exemplifies  
249 the power of having such a summary statistic, as different parameters and field sites can be rapidly  
250 and robustly compared. The information provided by the  $HI_{new}$  can be used in conjunction with other  
251 common metrics such as storm maximum concentration to produce a useful and robust quantitative  
252 representation of storm hydrochemical behaviour. Standardising approaches for the calculation of

253 HI would provide a useful tool for assessing storm behaviour. This is timely given the marked  
254 increase in the number of catchment scale water quality monitoring initiatives, which are now  
255 employing high temporal resolution monitoring to improve understanding of pollution sources and  
256 delivery pathways. Our ongoing research is exploring the use of this new index in understanding  
257 changing catchment dynamics associated with storm behaviours.

#### 258 *Acknowledgements*

259 The authors gratefully acknowledge the funding provided by Defra project WQ0211 (the Hampshire  
260 Avon Demonstration Test Catchment project) and NERC Grant NE/1002200/1 (The Environmental  
261 Virtual Observatory Pilot), and the access to the Brixton Deverill gauging site and flow data provided  
262 by Geoff Hardwicke at the Environment Agency.

263

264 Table 1: showing the increments of discharge measured and the corresponding number of storms  
265 (out of 66 analysed) and the percentage of storms which can be robustly\* characterised using  
266 different HI methods. \*Where adding extra measurement sections does not statistically change the  
267 distribution of HI vales for a storm.

Percentile increments	Sections measured	Storms ( $HI_L/HI_{LA}$ )	Storms ( $HI_{new}$ )
50%	1	5 (8%)	1 (1.5%)
25%	3	34 (52%)	41 (62%)
10%	9	55 (83%)	63 (95%)
5%	19	65 (98%)	66 (100%)
1%	99	66 (100%)	66 (100%)

268

269

270 5. References

271

272 Aich, V., Zimmermann, A., and Elsenbeer, H.: Quantification and interpretation of suspended-  
273 sediment discharge hysteresis patterns: How much data do we need?, *Catena*, 122, 120-129,  
274 10.1016/j.catena.2014.06.020, 2014.

275 Bowes, M. J., House, W. A., and Hodgkinson, R. A.: Phosphorus dynamics along a river continuum,  
276 *Science of the Total Environment*, 313, 199-212, 10.1016/s0048-9697(03)00260-2, 2003.

277 Bowes, M. J., Jarvie, H. P., Halliday, S. J., Skeffington, R. A., Wade, A. J., Loewenthal, M., Gozzard, E.,  
278 Newman, J. R., and Palmer-Felgate, E. J.: Characterising phosphorus and nitrate inputs to a rural river  
279 using high-frequency concentration-flow relationships, *The Science of the total environment*, 511,  
280 608-620, 10.1016/j.scitotenv.2014.12.086, 2015.

281 Burt, T. P., Worrall, F., Howden, N. J. K., and Anderson, M. G.: Shifts in discharge-concentration  
282 relationships as a small catchment recover from severe drought, *Hydrological Processes*, 29, 498-  
283 507, 10.1002/hyp.10169, 2015.

284 Butturini, A., Alvarez, M., Bernal, S., Vazquez, E., and Sabater, F.: Diversity and temporal sequences  
285 of forms of DOC and NO<sub>3</sub>-discharge responses in an intermittent stream: Predictable or random  
286 succession?, *J. Geophys. Res.-Biogeosci.*, 113, 10.1029/2008jg000721, 2008.

287 Cerro, I., Sanchez-Perez, J. M., Ruiz-Romera, E., and Antiguedad, I.: Variability of particulate (SS, POC)  
288 and dissolved (DOC, NO<sub>3</sub>) matter during storm events in the Alegria agricultural watershed,  
289 *Hydrological Processes*, 28, 2855-2867, 10.1002/hyp.9850, 2014.

290 Darwiche-Criado, N., Comin, F. A., Sorando, R., and Sanchez-Perez, J. M.: Seasonal variability of NO<sub>3</sub>-  
291 mobilization during flood events in a Mediterranean catchment: The influence of intensive  
292 agricultural irrigation, *Agriculture Ecosystems & Environment*, 200, 208-218,  
293 10.1016/j.agee.2014.11.002, 2015.

294 Eder, A., Strauss, P., Krueger, T., and Quinton, J. N.: Comparative calculation of suspended sediment  
295 loads with respect to hysteresis effects (in the Petzenkirchen catchment, Austria), *Journal of*  
296 *Hydrology*, 389, 168-176, 10.1016/j.jhydrol.2010.05.043, 2010.

297 Evans, C., and Davies, T. D.: Causes of concentration/discharge hysteresis and its potential as a tool  
298 for analysis of episode hydrochemistry, *Water Resources Research*, 34, 129-137,  
299 10.1029/97wr01881, 1998.

300 Evans, D. J., and Johnes, P.: Physico-chemical controls on phosphorus cycling in two lowland streams.  
301 Part 1 - the water column, *Science of the Total Environment*, 329, 145-163,  
302 10.1016/j.scitotenv.2004.02.016, 2004.

303 House, W. A., and Warwick, M. S.: Hysteresis of the solute concentration/discharge relationship in  
304 rivers during storms, *Water Research*, 32, 2279-2290, 10.1016/s0043-1354(97)00473-9, 1998.

305 Jarvie, H. P., Neal, C., Williams, R. J., Neal, M., Wickham, H. D., Hill, L. K., Wade, A. J., Warwick, A.,  
306 and White, J.: Phosphorus sources, speciation and dynamics in the lowland eutrophic River Kennet,  
307 UK, *Science of the Total Environment*, 282, 175-203, 10.1016/s0048-9697(01)00951-2, 2002.

308 Jordan, P., Arnscheidt, A., McGrogan, H., and McCormick, S.: Characterising phosphorus transfers in  
309 rural catchments using a continuous bank-side analyser, *Hydrology and Earth System Sciences*, 11,  
310 372-381, 2007.

311 Klein, M.: ANTI CLOCKWISE HYSTERESIS IN SUSPENDED SEDIMENT CONCENTRATION DURING  
312 INDIVIDUAL STORMS - HOLBECK CATCHMENT - YORKSHIRE, ENGLAND, *Catena*, 11, 251-257,  
313 10.1016/s0341-8162(84)80024-7, 1984.

314 Langlois, J. L., Johnson, D. W., and Mehuys, G. R.: Suspended sediment dynamics associated with  
315 snowmelt runoff in a small mountain stream of Lake Tahoe (Nevada), *Hydrological Processes*, 19,  
316 3569-3580, 10.1002/hyp.5844, 2005.

317 Lawler, D. M., Petts, G. E., Foster, I. D. L., and Harper, S.: Turbidity dynamics during spring storm  
318 events in an urban headwater river system: The Upper Tame, West Midlands, UK, *Science of the*  
319 *Total Environment*, 360, 109-126, 10.1016/j.scitotenv.2005.08.032, 2006.



320 Lloyd, C. E. M., Freer, J. E., Johnes, P. J., Coxon, G., and Collins, A. L.: Discharge and nutrient  
321 uncertainty: implications for nutrient flux estimation in small streams, *Hydrological Processes*, n/a-  
322 n/a, 10.1002/hyp.10574, 2015.

323 Lloyd, C. E. M., Freer, J. E., Johnes, P. J., and Collins, A. L.: Using hysteresis analysis of high-resolution  
324 water quality monitoring data, including uncertainty, to infer controls on nutrient and sediment  
325 transfer in catchments, *Science of The Total Environment*, 543, Part A, 388-404,  
326 <http://dx.doi.org/10.1016/j.scitotenv.2015.11.028>, 2016.

327 McDonald, D. M., and Lamoureux, S. F.: Hydroclimatic and channel snowpack controls over  
328 suspended sediment and grain size transport in a High Arctic catchment, *Earth Surface Processes and  
329 Landforms*, 34, 424-436, 10.1002/esp.1751, 2009.

330 McGonigle, D. F., Burke, S. P., Collins, A. L., Gartner, R., Haft, M. R., Harris, R. C., Haygarth, P. M.,  
331 Hedges, M. C., Hiscock, K. M., and Lovett, A. A.: Developing Demonstration Test Catchments as a  
332 platform for transdisciplinary land management research in England and Wales, *Environmental  
333 Science: Processes & Impacts*, 10.1039/C3EM00658A, 2014.

334 Oeurng, C., Sauvage, S., and Sanchez-Perez, J.-M.: Temporal variability of nitrate transport through  
335 hydrological response during flood events within a large agricultural catchment in south-west  
336 France, *Science of the Total Environment*, 409, 140-149, 10.1016/j.scitotenv.2010.09.006, 2010.

337 Outram, F. N., Lloyd, C. E. M., Jonczyk, J., Benskin, C. M. H., Grant, F., Perks, M. T., Deasy, C., Burke,  
338 S. P., Collins, A. L., Freer, J., Haygarth, P. M., Hiscock, K. M., Johnes, P. J., and Lovett, A. L.: High-  
339 frequency monitoring of nitrogen and phosphorus response in three rural catchments to the end of  
340 the 2011–2012 drought in England, *Hydrol. Earth Syst. Sci.*, 18, 3429-3448, 10.5194/hess-18-3429-  
341 2014, 2014.

342 Rodriguez-Blanco, M. L., Taboada-Castro, M. M., and Taboada-Castro, M. T.: Phosphorus transport  
343 into a stream draining from a mixed land use catchment in Galicia (NW Spain): Significance of runoff  
344 events, *Journal of Hydrology*, 481, 12-21, 10.1016/j.jhydrol.2012.11.046, 2013.

345 Tena, A., Vericat, D., and Batalla, R. J.: Suspended sediment dynamics during flushing flows in a large  
346 impounded river (the lower River Ebro), *Journal of Soils and Sediments*, 14, 2057-2069,  
347 10.1007/s11368-014-0987-0, 2014.

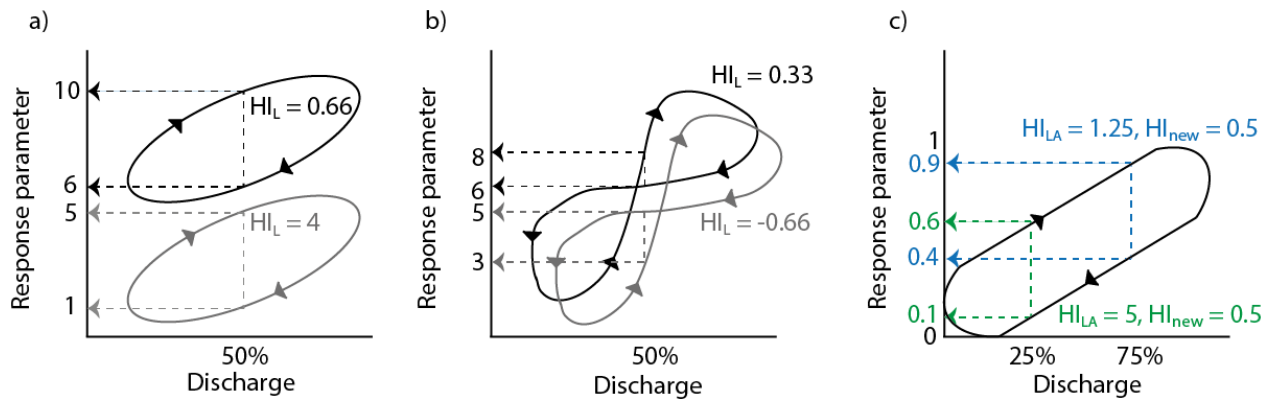
348 Whiting, P. J., Samm, J. F., Moog, D. B., and Orndorff, R. L.: Sediment-transporting flows in  
349 headwater streams, *Geological Society of America Bulletin*, 111, 450-466, 10.1130/0016-  
350 7606(1999)111<0450:stfihs>2.3.co;2, 1999.

351 Williams, G. P.: Sediment concentration versus water discharge during single hydrologic events in  
352 rivers, *Journal of Hydrology*, 111, 89-106, 10.1016/0022-1694(89)90254-0, 1989.

353 Ziegler, A. D., Benner, S. G., Tantasirin, C., Wood, S. H., Sutherland, R. A., Sidle, R. C., Jachowski, N.,  
354 Nullet, M. A., Xi, L. X., Snidvongs, A., Giambelluca, T. W., and Fox, J. M.: Turbidity-based sediment  
355 monitoring in northern Thailand: Hysteresis, variability, and uncertainty, *Journal of Hydrology*, 519,  
356 2020-2039, 10.1016/j.jhydrol.2014.09.010, 2014.

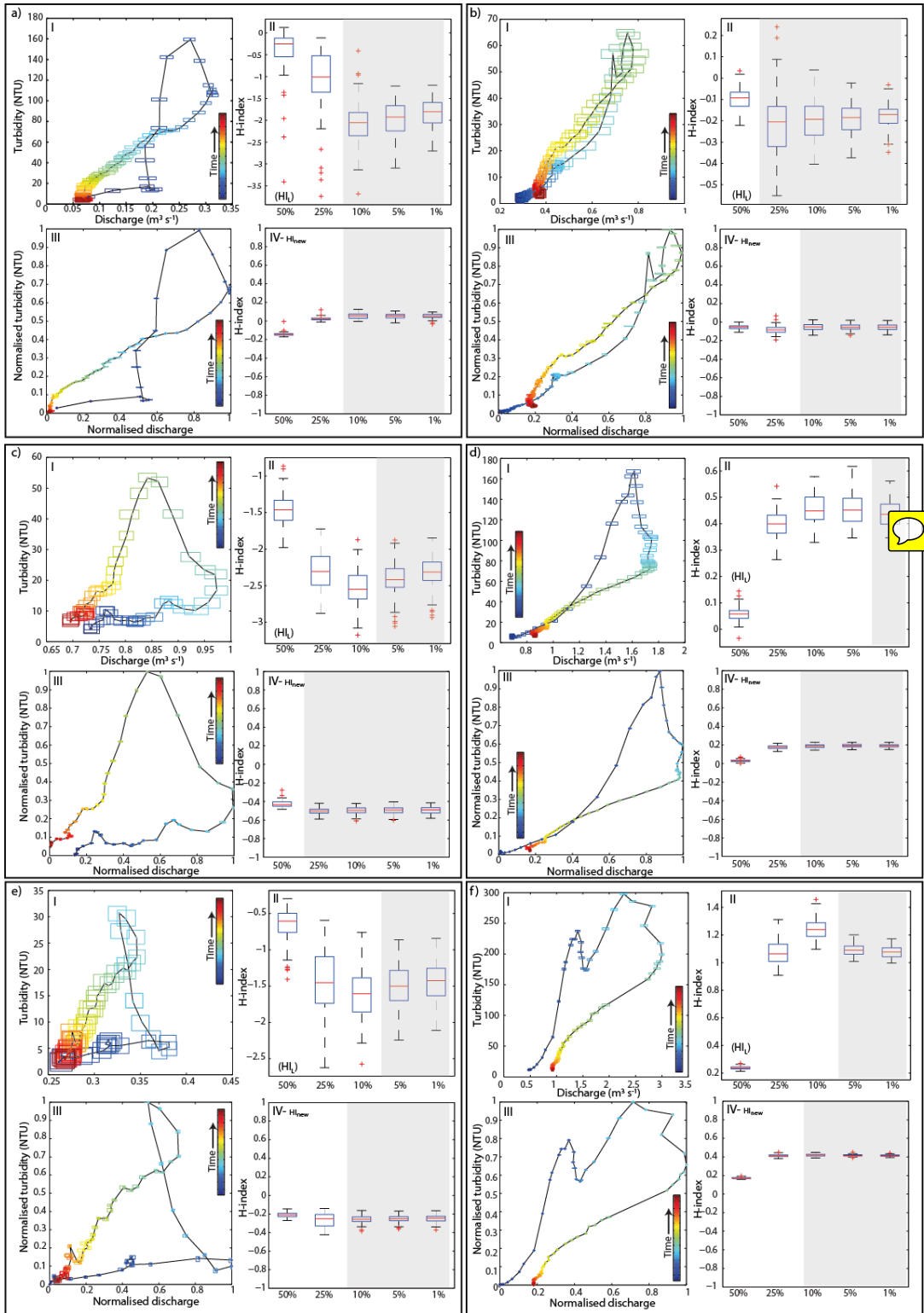
357

358



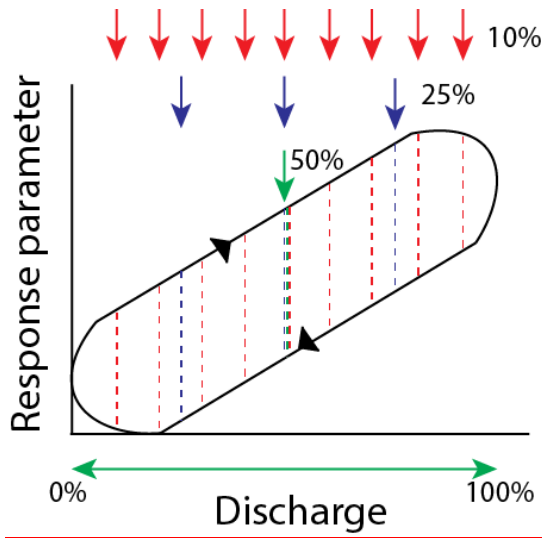
359

360 Figure 1: Plots showing a) impact of storm initial concentration, b) storm initial discharge on the  
 361 value of the calculated HI when the mid-point in discharge and raw data is used and c) an idealised  
 362 and normalised storm illustrating the impact of measuring different quantiles of flow on the HI  
 363 calculated. Where  $HI_L$  and  $HI_{LA}$  are the original and adapted Lawler et al. (2006) methods,  
 364 respectively and  $HI_{new}$ , the proposed new method. Colours represent different discharge intervals  
 365 measured.



366

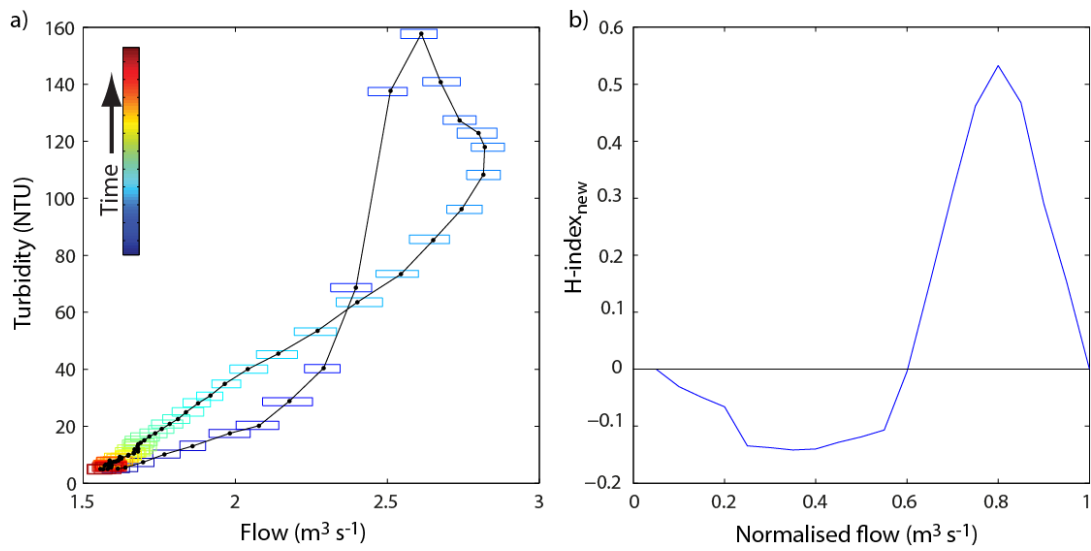
367 Figure 2: Plots showing six storms with varying loop shapes and sizes (a-f), where (I) is the hysteresis  
 368 loop using the raw data, (II) is the distribution of HI values using the original and adapted Lawler et  
 369 al. (2006) methods ( $HI_L/HI_{LA}$ ) using varying percentiles of flow, (III) is the hysteresis loop plotted using  
 370 normalised data, and (IV) is the distribution of HI values using the new method ( $HI_{new}$ ) using varying  
 371 percentiles of flow. The grey areas show the distributions which are not statistically different from  
 372 each other. In panels I and III, the black line represents the median and the boxes represent the 5<sup>th</sup>-  
 373 95<sup>th</sup> percentiles of the uncertainty range.



374

375 **Figure 3:** diagram showing examples of how the sampling intervals for the calculation of the  $HI_{LA}$  and  
 376  $HI_{new}$  are determined.

377



378

379 | Figure 43: showing a) the original storm, where the black line represents the median  
 380 | the 5<sup>th</sup>-95<sup>th</sup> percentiles of the uncertainty around the line, and b) illustrates the  $H\text{-index}_{\text{new}}$  of the  
 381 | normalised storm.